

Models for the Nearfield Interaction of a Magnetic Field From Point Sources Representing Transformers and Power Supplies and a Ferromagnetic Cylindrical Shell

Dr. Theodore R. Anderson
Naval Undersea Warfare Center Detachment
New London, CT 06320

Abstract — This paper describes models of the magnetic field interactions from various sources and a physical blockage. The sources represent power supplies, transformers, and cables; the physical blockage is a cylindrical shell. The sources are modeled as vector fields in the magnetostatic limit. Boundary conditions applied at the outer and inner interfaces of the cylindrical shell require that the normal component of the B field and the tangential component of the H field be continuous at the outer and inner interfaces. The source fields are transformed to the coordinate system of the cylindrical shell, where the final solutions are given. The source fields are expanded in binomial expansions, and the response fields outside, within, and in the interior region of the cylindrical shell are expanded in Legendre polynomial expansions. Upon application of the boundary conditions, a system of linear equations is generated by matching powers of sine and cosine functions in the binomial and Legendre polynomial expansions. The solutions of this system of equations yield the coefficients of expansion of the Legendre polynomials. The number of equations generated depends on the extent of the expansions, which, in turn, depends on the accuracy that is required. After solving for the coefficients of expansion, the coefficients are substituted back into the Legendre polynomial field equations, and the gradients are taken to obtain the vector fields. These fields are then added to the source fields to obtain the final solutions.

INTRODUCTION

This effort was designed to improve electromagnetic analysis techniques that can be used to supplement the Intelligent EMC Analysis and Design System (IEMCADS) [1]. IEMCADS uses such sources as transformers, cables, and power supplies, which are represented in a simplistic and scalar form to yield worst-case field conditions. These sources do not give rise to uniform fields or plane waves, but to fields that vary as inverse powers of the radial distance.

It was decided that the best way to obtain an analytical solution to this problem was to expand the sources that exist in IEMCADS in Legendre polynomials and use a hollow cylindrical physical blockage as a representation of cabinets. This technique will enable the fields in the various regions around and within the physical blockage to be modeled as expansions in Legendre polynomials [2]-[6]. These expansions make the source modeling compatible with the physical blockage modeling, and hence boundary conditions can be applied for the B and H fields at the two interfaces of the cylindrical shell. The application of the boundary conditions generates a system of 10 equations and 10 unknowns for the coefficients of expansion for each source type. The solution of the 10 equations and 10 unknowns yields the coefficients of expansion of the Legendre polynomials. The final Legendre polynomial expansions yield the magnetic scalar potentials for the different sources. The gradients of the magnetic scalar potentials are then taken to yield the vector B and H fields in the regions of the source, the regions outside and within the shell of the physical blockage, and the hollow region of the physical blockage.

THE MATHEMATICAL MODELS

The IEMCADS power supply field varies as $1/|\bar{r}-\bar{r}'|$ and the IEMCADS transformer field varies as $1/|\bar{r}-\bar{r}'|^3$. From figure 1, \bar{r}' is the distance from the source to the center of the cylindrical shell and \bar{r} is the distance from the cylindrical axis to the point of observation. The coordinates of the point of observation are always \bar{r} and θ .

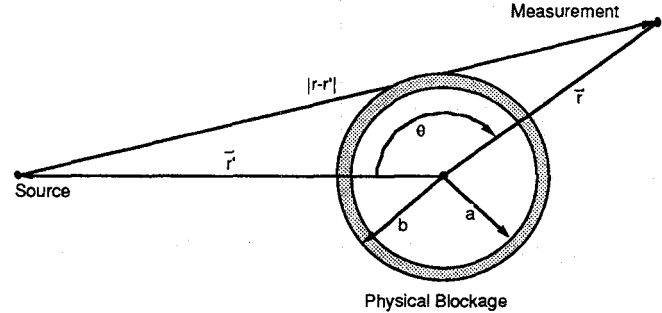


Figure 1. Representation of the Physical Blockage

General Method for Application of the Boundary Conditions

The coefficients of the Legendre polynomial expansions [4] are solved by the application of the boundary conditions at the two interfaces: $r = a$ and $r = b$. These boundary conditions are the continuity of the tangential components of the H field and the normal components of the B field. To apply these boundary conditions requires that the coefficients of $(\cos^n)(\sin^m)$, where $n = 0, 1, 2$ and $m = 0, 1, 2$, are set equal to zero.

The application of the boundary conditions involved two cases: $\bar{r} \geq \bar{r}'$ and $\bar{r} \leq \bar{r}'$. The coefficients of expansion of the Legendre polynomials are different for these two cases since the sources are expanded as a binomial expansion in powers of r'/r for the case $r \geq r'$ and in powers of r/r' for the case $r \leq r'$. (Physically, the case $r \geq r'$ means that the source is closer to the physical blockage than to the point of observation, and the case $r' \geq r$ means that the point of observation is closer to the physical blockage than to the source.) The binomial expansions of the sources are necessary to obtain coefficients of powers of sines and cosines. These expansions can then be combined with the Legendre polynomial expansions to generate the 10 equations and 10 unknowns. The 10 equations yield unique solutions for the 10 unknowns, which are then substituted back into equations (1), (2), and (3) below. The gradient operations were carried out in the three equations to yield the general solutions.

The Mathematical Form for the $1/|\bar{r}-\bar{r}'|$ Source

The H fields are given in three regions: $r > b$, $a < r < b$, and $r < a$. For $r > b$, the H field is given by

$$\vec{H} = \frac{B_0}{|\bar{r}-\bar{r}'|} \frac{(\bar{r}-\bar{r}')}{|\bar{r}-\bar{r}'|^3} - \nabla \sum_{\ell=0}^2 \frac{\alpha_{\ell}}{r^{\ell+1}} P_{\ell}(\cos(\theta)). \quad (1)$$

For $a < r < b$,

$$\vec{H} = -\nabla \sum_{\ell=0}^2 \left(\beta_{\ell} r^{\ell} + \frac{\gamma_{\ell}}{r^{\ell+1}} P_{\ell}(\cos(\theta)) \right), \quad (2)$$

and for $r < a$,

$$H = -\nabla \sum_{\ell=0}^2 \delta_{\ell} r^{\ell} P_{\ell}(\cos(\theta)). \quad (3)$$

Expanding equations (1), (2), and (3) yields for $r > b$

$$\begin{aligned} \bar{H} = \hat{r} & \left[\frac{B_0}{r^2 + r'^2 - 2rr'} (r - r' \cos \theta) - \frac{\alpha_1}{r^2} \cos \theta \right. \\ & \left. + \frac{\alpha_0}{r^2} + \frac{3\alpha_2}{2r^4} (3 \cos^2 \theta - 1) \right] \\ & + \hat{\theta} \left[\frac{B_0 r' \sin \theta}{r^2 + r'^2 - 2rr'} - \frac{\alpha_1}{r} \sin \theta + \frac{\alpha_2}{2r^4} (6 \cos \theta \sin \theta) \right]; \end{aligned} \quad (4)$$

for $b > r > a$

$$\begin{aligned} \bar{H} = \hat{r} & \left[\left(\gamma_1 \frac{2}{r^3} - \beta_1 \right) \cos \theta + \frac{\gamma_0}{r^2} + \left(\gamma_2 \frac{3}{r^4} + 2\beta_2 r \right) (3 \cos^2 \theta - 1) \right] \\ & + \hat{\theta} \left[\left(\beta_1 + \frac{\gamma_1}{r^3} \right) \sin \theta - \beta_2 r + \frac{6\gamma_2}{r^4} \sin \theta \cos \theta \right]; \end{aligned} \quad (5)$$

and for $r < b$

$$\begin{aligned} \bar{H} = \hat{r} & \left[\frac{2\delta_1}{r^3} \cos \theta - \frac{3\delta_2}{4r^4} (3 \cos^2 \theta - 1) + \frac{\delta_0}{r^2} \right] \\ & + \hat{\theta} \left[\frac{\delta_1}{r^3} \sin \theta + \frac{3\delta_2}{r^4} \sin \theta \cos \theta \right]. \end{aligned} \quad (6)$$

The $1/|\bar{r} - \bar{r}'|$ Source in Component Form and

Its Binomial Expansion

The B field for the $1/|\bar{r} - \bar{r}'|$ source can be expressed as

$$B = \frac{B_0}{|\bar{r} - \bar{r}'|} \frac{(\bar{r} - \bar{r}')}{|\bar{r} - \bar{r}'|}, \quad (7)$$

where the second factor is the unit vector extending from the source to the observation point (experimental point). Taking the dot product of B with the unit vectors in the radial and angular directions of the physical blockage cylindrical coordinate system yields

$$B_r = \frac{B_0}{|\bar{r} - \bar{r}'|} \frac{(\bar{r} - \bar{r}') \cdot \bar{r}}{|\bar{r} - \bar{r}'|} = \frac{B_0}{|\bar{r} - \bar{r}'|^2} (r - r' \cos \theta) \quad (8)$$

and

$$B_{\theta} = \frac{B_0}{|\bar{r} - \bar{r}'|^2} (\bar{r} - \bar{r}') \cdot \hat{\theta} = B_0 \frac{r' \sin \theta}{|\bar{r} - \bar{r}'|^2}. \quad (9)$$

Expanding $1/|\bar{r} - \bar{r}'|^2$ in the binomial expansion yields

$$1/|\bar{r} - \bar{r}'|^2 \approx \frac{1}{r^2} \left(1 - \frac{r'^2}{r^2} + \frac{2r'}{r} \cos \theta \right) \quad \text{for } \bar{r} \geq \bar{r}' \quad (10)$$

and

$$1/|\bar{r} - \bar{r}'|^2 \approx \frac{1}{r'^2} \left(1 - \frac{r^2}{r'^2} + \frac{2r}{r'} \cos \theta \right) \quad \text{for } \bar{r} \leq \bar{r}'. \quad (11)$$

The Mathematical Solution of the B and H Fields for the

$1/|\bar{r} - \bar{r}'|$ Source

We substitute equations (10) and (11) into equations (8) and (9) and the result into the source terms of equations (1), (2), and (3). By applying the boundary conditions for the B and H fields to the resulting equations and setting the coefficients of the powers of the sines and cosines equal to zero, we generate the 10 equations and 10 unknowns, which are solved to obtain the expansion coefficients. These coefficients are then substituted back into equations (1), (2), and (3) to yield a numerical solution.

The Mathematical Form for the $1/|\bar{r} - \bar{r}'|^3$ Source

The H fields are given in three regions: $r > b$, $a < r < b$, and $r < a$.

For $r > b$, the H field is given by

$$\bar{H} = \frac{B_0}{|\bar{r} - \bar{r}'|^3} \frac{(\bar{r} - \bar{r}')}{|\bar{r} - \bar{r}'|} - \nabla \sum_{\ell=0}^2 \frac{\alpha_{\ell}}{r^{\ell+1}} P_{\ell}(\cos(\theta)); \quad (12)$$

for $a < r < b$,

$$\bar{H} = -\nabla \sum_{\ell=0}^2 \left(\beta_{\ell} r^{\ell} + \frac{\gamma_{\ell}}{r^{\ell+1}} \right) P_{\ell}(\cos(\theta)); \quad (13)$$

and for $r < a$,

$$\bar{H} = -\nabla \sum_{\ell=0}^2 \delta_{\ell} r^{\ell} P_{\ell}(\cos(\theta)). \quad (14)$$

Expanding equations (12), (13), and (14) yields for $r > b$

$$\begin{aligned} \bar{H} = \hat{r} & \left[\frac{B_0}{(r^2 + r'^2 - 2rr')^2} (r - r' \cos \theta) - \frac{\alpha_1}{r^2} \cos \theta + \frac{\alpha_0}{r^2} + \frac{3\alpha_2}{2r^4} (3 \cos^2 \theta - 1) \right] \\ & + \hat{\theta} \left[\frac{B_0 r' \sin \theta}{(r^2 + r'^2 - 2rr')^2} - \frac{\alpha_1}{r} \sin \theta + \frac{\alpha_2}{2r^4} (6 \cos \theta \sin \theta) \right]; \end{aligned} \quad (15)$$

for $b > r > a$

$$\begin{aligned} \bar{H} = \hat{r} & \left[\left(\gamma_1 \frac{2}{r^3} - \beta_1 \right) \cos \theta + \frac{\gamma_0}{r^2} + \left(\gamma_2 \frac{3}{r^4} + 2\beta_2 r \right) (3 \cos^2 \theta - 1) \right] \\ & + \hat{\theta} \left[\left(\beta_1 + \frac{\gamma_1}{r^3} \right) \sin \theta - \beta_2 r + \frac{6\gamma_2}{r^4} \sin \theta \cos \theta \right]; \end{aligned} \quad (16)$$

and for $r < b$

$$\vec{H} = \vec{r} \left[\frac{2\delta_1}{r^3} \cos \theta - \frac{3\delta_2}{4r^4} (3 \cos^2 \theta - 1) + \frac{\delta_0}{r^2} \right] + \hat{\theta} \left[\frac{\delta_1}{r^3} \sin \theta + \frac{3\delta_2}{r^4} \sin \theta \cos \theta \right]. \quad (17)$$

The $1/|\vec{r} - \vec{r}'|^3$ Source in Component Form and Its Binomial Expansion

The B field for the $1/|\vec{r} - \vec{r}'|^3$ can be expressed as

$$B = \frac{B_0}{|\vec{r} - \vec{r}'|^3} \frac{(\vec{r} - \vec{r}')}{|\vec{r} - \vec{r}'|}, \quad (18)$$

where the second factor is the unit vector extending from the source to the observation point (experimental point). Taking the dot product of B with the unit vectors in the radial and angular directions of the physical blockage cylindrical coordinate system yields

$$B_r = \frac{B_0}{|\vec{r} - \vec{r}'|^3} \frac{(\vec{r} - \vec{r}')}{|\vec{r} - \vec{r}'|} \cdot \vec{r} = \frac{B_0}{|\vec{r} - \vec{r}'|^4} (r - r' \cos \theta) \quad (19)$$

and

$$B_\theta = \frac{B_0}{|\vec{r} - \vec{r}'|^4} (\vec{r} - \vec{r}') \cdot \hat{\theta} = B_0 \frac{r' \sin \theta}{|\vec{r} - \vec{r}'|^4}. \quad (20)$$

Expanding $1/|\vec{r} - \vec{r}'|^4$ in the binomial expansion yields

$$\frac{1}{|\vec{r} - \vec{r}'|^4} \approx \frac{1}{r^4} \left(1 - 2 \left(\frac{r'^2}{r^2} - \frac{2r'}{r} \cos \theta \right) \right) \text{ for } \vec{r} \geq \vec{r}' \quad (21)$$

and

$$\frac{1}{|\vec{r} - \vec{r}'|^4} \approx \frac{1}{r'^4} \left(1 - 2 \left(\frac{r^2}{r'^2} - \frac{2r}{r'} \cos \theta \right) \right) \text{ for } \vec{r} \leq \vec{r}'. \quad (22)$$

The Mathematical Solution of the B and H Fields for the

$1/|\vec{r} - \vec{r}'|^3$ Source

We substitute equations (21) and (22) into equations (19) and (20) and the result into the source terms of equations (12), (13), and (14). By applying the boundary conditions for the B and H fields to the resulting equations and setting the coefficients of the powers of the sines and cosines equal to zero, we generated the 10 equations and 10 unknowns, which were solved to obtain the expansion coefficients. These coefficients are then substituted back into equations (12), (13), and (14) to yield a numerical solution.

The Mathematical Solution of the B and H Fields for the

$1/|\vec{r} - \vec{r}'|$ Cable Source

The cable source is perpendicular to the radial field source and is of the same magnitude. The cable source field in the presence of the physical blockage was solved with the binomial and Legendre polynomial expansions in the same way that the solutions for the previous two sources presented in this paper were obtained [5]. The solution to the fields at $\theta = 0$ yields disturbance fields, which are functions of angular derivatives

of the Legendre polynomials. The angular derivatives of the Legendre polynomials yield the angular component of the disturbance field, and, upon taking the derivatives, each term has a sine θ factor. Setting $\theta = 0$ yields zero for the disturbance field. The experiments made at $\theta = 0$ proved this to be true, as shown in figure 2.

EXPERIMENTS

The experiment was set up to measure the B and H fields from a wire with its axis parallel to the cylindrical shell blockage. This configuration produced an angular field, which varied as $1/|\vec{r} - \vec{r}'|$ from the source. The results of measurements taken at $\theta = 0$ and $\theta = \pi$ (figure 2) show a negligible amount of angular field disturbance, which decreased as the frequency decreased. The model predicts zero angular disturbance effect in the magnetostatic limit. Thus, the measurements are compatible with the model for this experimental configuration and these angles. The slight increase in the angular field disturbance as the frequency increased can be explained as an eddy current-Lenz law response of the physical blockage to the source field.

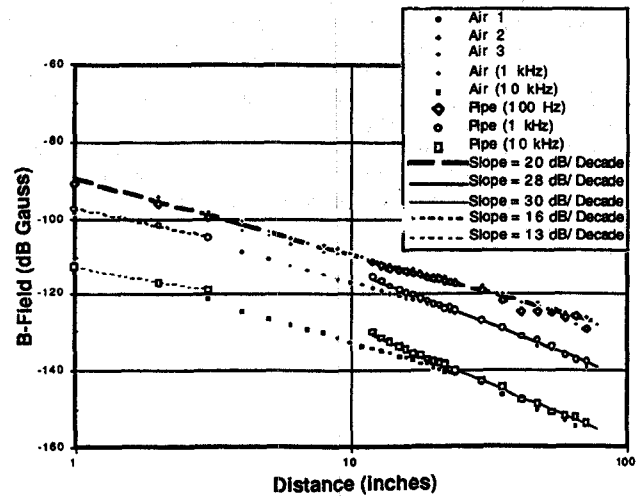


Figure 2. Measured Magnetic Field From a Straight Wire Near an Iron Pipe

CONCLUSIONS

The theoretical model for the angular field from a cable source predicted no physical distortion of the angular component magnetic field at $\theta = 0$ and $\theta = \pi$ with respect to the axis of the physical blockage (see figure 1). The distortion of the angular component of the magnetic field was calculated by taking the angular derivative of the Legendre polynomial expansion. After these derivatives were taken, each term in the Legendre polynomial expansion had a sine θ factor. Hence, the disturbance will vanish at $\theta = 0$ and $\theta = \pi$. Experimental measurements of the angular components of the magnetic field confirmed this (see the experimental plots on figure 2).

The theoretical model also predicted a periodicity with higher harmonics in the disturbance field, and, in fact, the disturbance field will vanish altogether on certain axes and be maximized on others. Besides the angular disturbance caused by a physical blockage on the angular field, the radial disturbance can be predicted by taking the radial derivatives of the Legendre polynomial expansion.

The other models developed were for the vector radial field sources that varied in inverse proportion to the distance and cube of the distance. These sources, represented in the EMC code called IEMCADS as power supplies and transformers, are simplistically treated by the IEMCADS code as scalars; however, to solve for the distortion effects of the physical blockage on the source fields, the sources had to be treated as vectors in

order to apply the boundary conditions that require the angular component of the H field and the normal component of the B field to be continuous at the inner and outer interfaces. Upon application of the boundary conditions, a set of 10 equations and 10 unknowns was derived and solved to obtain the expansion coefficients for the Legendre polynomials, which resulted in a net field as demonstrated in this paper. Although these particular cases were not checked in the laboratory since the mathematical sources are severe approximations to real power supplies and transformers, the mathematical sources developed (being vector fields) are an improvement over the sources used in IEMCADS. Realistically, the nearfields from transformers and power supplies have both radial and angular components with coefficients in spherical coordinates.

In summary, the goal in this investigation was to develop models to improve IEMCADS by incorporating the physical blockage. This meant keeping the source models as close to the IEMCADS models as possible. We could not, however, use the IEMCADS scalar fields designed to predict worst-case field conditions because the boundary conditions at the physical blockage could not be applied. Although the complexity of the nearfield complicated the process, we reconstructed sources in IEMCADS to give them a vector nature with more physical reality.

Future work should focus on the development of complete nearfield models for transformers and power supplies other than on the approximate models developed here. The same techniques described earlier for determining the effects of physical blockage should be applied to these improved source models, and experiments to validate the models should be conducted. The source model used for the cables in this study was exact and requires no improvement. However, experimental measurements of the effects of the physical blockage at angles other than $\theta = 0$ and $\theta = \pi$ should be undertaken.

ACKNOWLEDGMENTS

This paper was prepared with support from the Naval Sea Systems Command's *Below Decks EM Emergency Program*, Program Manager Donald Cebulski (NAVSEA 03K2) and Principal Investigator William Douglas (NAVSEA 03K41). The Naval Undersea Warfare Center's Program Manager for this effort was David S. Dixon. The author also acknowledges Nicholas Schade for his assistance with the experiment.

REFERENCES

- [1] "Intelligent EMC Analysis and Design System (IEMCADS)," Report No. KSC-WO3132N, Kaman Sciences Corporation, Utica, NY, 1993.
- [2] G. Arfken, *Mathematical Methods for Physicists*. New York: Academic Press, Inc., 1985, Third Edition, pp. 637-707.
- [3] L. Bailin and S. Silver, "Exterior Electromagnetic Boundary Value Problems for Spheres and Cones," *IEEE Transactions on Antennas and Propagation*, vol. AP-4, no. 1, p. 15, 1956.
- [4] D. Jackson, *Classical Electrodynamics*. New York: John Wiley & Sons, Inc., 1962, First Edition.
- [5] T. Anderson, "Magnetic Field Intensity Due To a Line of Current of Arbitrary Orientation in Cartesian Coordinates," NUWC-NPT Technical Memorandum 941145, Naval Undersea Warfare Center Detachment, New London, CT, 23 November 1994.
- [6] J. Reitz and F. Milford, *Foundations of Electromagnetic Theory*, Reading, MA: Addison-Wesley Publishing Company, Inc., 1967.